J. Braz. Chem. Soc., Vol. 13, No. 1, 47-53, 2002.
Printed in Brazil - ©2002 Sociedade Brasileira de Química
0103 - 5053 $6.00+0.00

Article

Temporal Evolution of Soot Particles from C_2H_2/O_2 Combustion in a Closed Chamber

Celso A. Bertran*, Carla S. T. Marques and Leandro H. Benvenutti

Instituto de Química, Universidade Estadual de Campinas, CP 6154, 13083-970, Campinas - SP, Brazil.

Neste trabalho, realizou-se um estudo da formação de partículas de fuligem durante a combustão de misturas de C_2H_2/O_2 em diferentes razões C/O. A evolução temporal e a fração de volume das partículas de fuligem foram obtidas através da extinção de um feixe de laser.

Constatou-se que o tempo total de formação da fuligem nas chamas de C_2H_2/O_2 com razão C/O > 0.75 ou de C_2H_2/O_2/Ar com razão C/O = 1.00 é de cerca de 3.0-4.0 ms, após o início da reação. O máximo de emissão dos radicais excitados e o máximo da pressão nestas reações, ocorrem praticamente neste mesmo intervalo de tempo. Observou-se a formação de partículas de fuligem compactas e aproximadamente esféricas com 60-150 nm de diâmetro. Entretanto, os agregados não são compactos e mostram uma estrutura de rede que se assemelha a de um aerogel.

An experimental study of soot formation in C_2H_2/O_2 flames at different C/O ratios in a closed chamber was carried out. The evolution temporal behavior and the volume fraction of soot particles were determined by laser extinction.

It was found that total time for the soot formation phenomenon in flames from C_2H_2/O_2 with C/O ratio > 0.75 or C_2H_2/O_2/Ar with C/O ratio = 1.00 was around 3.0-4.0 ms after ignition. At almost the same time the excited radicals reached their maximum emission intensity and the gases under combustion reached their maximum pressure. The micrographs show compact and approximately spherical soot particles with diameters within 60-150 nm. However, soot aggregates are not compact and they present a netlike structure similar to that of an aerogel.

Keywords: soot formation, closed chamber, combustion, laser extinction

Introduction

In recent years, soot formation in hydrocarbon flames has been intensively studied, due to the numerous types of soot-containing flames as well as the environmental implications.[1-5] Heat transfer rates and, therefore, the efficiency of the most practical combustion systems, such as gas turbines, internal combustion engines, boilers, industrial furnaces and fires, are strongly affected by the presence of soot.[2,6] Furthermore, the emission of fine particles (organic carbon aerosols and soot) into the atmosphere, generated by combustion systems, is directly related to respiratory illness and mortality.[7,8]

The chemistry of soot formation is a very complex phenomenon involving homogeneous and heterogeneous processes and the continuous competition between formation and oxidation reactions.[9]

The overall mechanism of soot production is normally described as three steps: nucleation, surface growth and coalescence, then aggregation.[9,10] The particle surface growth has been found to dominate soot mass yield, which progresses via hydrogen abstraction, creating a surface radical site in preparation for carbon addition by principally, C_2H_2 molecules to the site (the HACA, hydrogen-abstraction/carbon-addition, mechanism).[4,11]

Soot particles emitted from combustion systems consist of chainlike aggregates of spherical units having hexagonal structures similar to graphite and having, generally, diameters of 10-50 nm.[12] Particle sizes and the morphology of soot are characteristic of the nature of original fuel and its oxidation products.[13]

Acetylene is one of the major intermediates in almost all hydrocarbon flames.[14] Its combustion has been extensively reported in the literature and can be used as a model for other combustion and soot formation processes.

However, the mechanisms of soot formation have not been fully established yet and the difficulty is to understand the rapid growth of primary particles into soot particles of 10-50 nm diameters.

In such aspects, the accurate determination of the temporal evolution of soot particles is very important to

* e-mail: bertran@iqm.unicamp.br

understand soot chemistry and its influence on combustion systems. The kinetics of soot production provides useful information for simulation studies of soot formation mechanisms and soot formation control.

However, most research has been conducted in open systems of atmospheric laminar flames in which the temporal growth of soot particles could only be estimated.

Several soot diagnostic techniques have been employed in combustion research. Light extinction is one the most widely applied techniques for soot diagnostics.[4,5,7,15,16] The attenuation of light caused by the sum of scattering and absorption by the particles provides a measure of the soot volume fraction. Laser-induced incandescence is another diagnostic tool for soot concentration and particle size measurements.[11,17-19] Soot particle sizes have also been determined by scanning and transmission electron microscopy analyses.[1,2,4,16,20,21]

The proposal of this work is to study the temporal behavior of the initial steps of soot formation: nucleation, surface growth and coalescence and, the temporal evolution of the volume fraction from C_2H_2/O_2 combustion in a closed chamber. Combustion in closed chambers more closely resembles that of internal combustion engines and allows the study of combustion with well-defined quantities of all reagents, without the influence of the surroundings.

The temporal behavior of the evolution and the volume fraction of soot particles were established by laser extinction and the morphology of these particles was analyzed by scanning electron microscopy. The measurements were carried out for C_2H_2/O_2 combustion at different C/O ratios and, in order to evaluate the effect of inert gas addition on the soot formation mechanism, argon was added to a C_2H_2/O_2 flame with C/O ratio = 1.00. The soot precursors are mainly polycyclic aromatic hydrocarbons (PAH)[10,22] and argon could influence the reaction kinetics of soot formation from these species with high molecular mass.

Chemiluminescence of excited radicals and pressure changes were also obtained for these combustion reactions. The results of chemiluminescence and pressure measurements were obtained independently of the laser extinction measurements and they allowed determination of the evolution of soot formation within the total time of the combustion process.

Experimental

Experimental combustion system

Figure 1 shows the experimental setup for combustion analysis. It consists of a cylindrical closed chamber, a pressure transducer, a light source, an optical arrangement and a digital oscilloscope.

The combustion chamber has a 200 mL volume: 18 cm length, 3.4 cm internal diameter and 7.5 cm external diameter. To start the combustion process, a spark plug was attached at the center of the chamber wall. In order to allow light detection, both ends of the combustion chamber were closed by acrylic windows 1 cm thick. All gaseous mixtures were prepared directly in the closed chamber by means of a vacuum manifold. They were kept there for 30 min before the ignition process.

A helium-neon laser of 5 mW power was the light source for light extinction measurements to study soot formation. The laser beam was directed at the central axis of the combustion chamber and it was detected and analyzed by an optical system. The optical system is

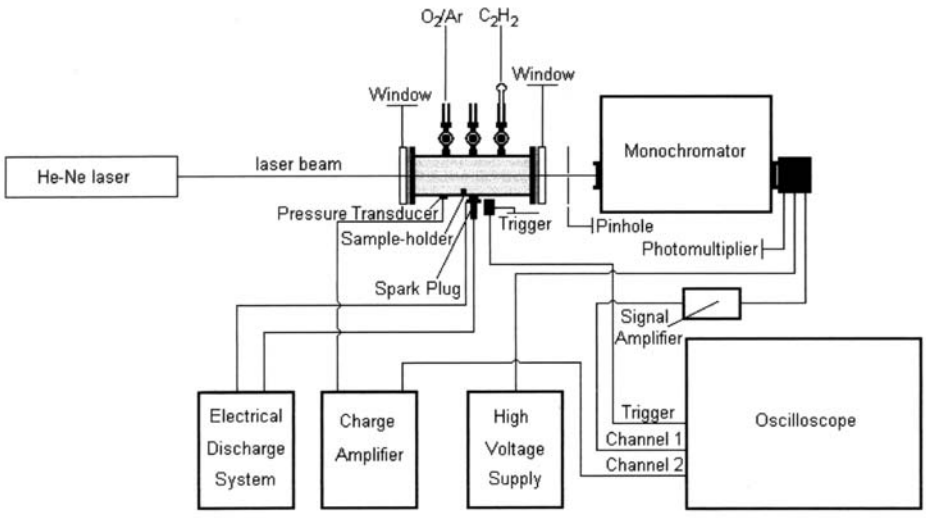

Figure 1. Experimental setup for soot formation analysis in the C_2H_2/O_2 and C_2H_2/O_2/Ar flames.

Table 1. Experimental conditions of C_2H_2/O_2 e C_2H_2/O_2/Ar flames analyzed by laser extinction measurements.

	P_{Total} / mmHg	P_{C2H2} / mmHg	P_{O2} / mmHg	P_{Ar} / mmHg	C/O ratio
Mixture 1	140	55	85	-	0.65
Mixture 2	140	60	80	-	0.75
Mixture 3	140	63	77	-	0.82
Mixture 4	140	65	75	-	0.87
Mixture 5	140	70	70	-	1.00
Mixture 6	210	70	70	70	1.00

composed of pinholes of 1 mm, slits and a 0.25 m monochromator coupled to a photomultiplier. An oscilloscope was used to record the change of laser intensity. The digital oscilloscope was pre-triggered 2 ms before starting the combustion by a home made electrical discharge system to measure the I_0 intensity at 632.8 nm. In this optical configuration, the light emission from combustion at the 632.8 nm wavelength was negligible, compared to intensity of the laser light.

Soot particles were collected in a sample-holder, placed inside the combustion chamber, using the thermophoretic sampling method.[1,2] The sample-holder works as a cold metallic surface, where the soot particles are deposited. After particle collection, the sample was coated with gold. Scanning electron microscopy was carried out to determine both the soot particle diameters and the aggregation structure by using a JEOL type T 300 microscope.

Combustion propagation was monitored by pressure measurements by using a KISTLER type 601A pressure transducer connected to a KISTLER type 5011B charge amplifier. Chemiluminescence measurements were performed using a photomultiplier.

Experimental conditions

The experimental conditions are summarized in Table 1. Soot particle formation was studied for C_2H_2/O_2 flames in the C/O ratio range between 0.65 and 1.00 and for C_2H_2/O_2/Ar flames with C/O ratio = 1.00 (mixture 6) by laser extinction measurements. Pressure measurements and scanning electron microscopy analyses were only obtained for C_2H_2/O_2 and C_2H_2/O_2/Ar flames with C/O ratio = 1.00 (mixtures 5 and 6), due to the large soot yield in these flames. Chemiluminescence measurements of excited radicals OH ($A^2\Sigma \rightarrow X^2\Pi$), CHO ($A^2\Pi \rightarrow X^2A'$), CH ($A^2\Delta \rightarrow X^2\Pi$) and C_2 ($A^3\Pi \rightarrow X^3\Pi$) at their corresponding emission maxima, 306.4, 318.6, 431.3 and 516.5 nm[23], were also carried out for these both flames with C/O ratio = 1.00. The experimental setup used for chemiluminescence analysis[24] was similar to that in Figure 1. The He-Ne laser was turned off and the monochromator entrance slit (without pinholes) was placed directly at one of the windows to avoid stray light.

Data acquisition

Each type of measurement (laser extinction, pressure and chemiluminescence) was repeated three or more times for each combustion mixture presented in Table 1. Figure 2 shows an example of five independent measurements (oscilloscope records) of laser extinction for combustion processes of C_2H_2/O_2 with C/O = 1.00 (mixture 5). The records were superimposed and were smoothed after applying a mathematical filter of *Microcal Origin* 5.0, which utilizes Fourier Transformation (solid line in Figure 2). Figure 2 also shows the smoothed data of pressure change measurements inside the chamber.

Plots such as those shown in Figure 2 were obtained for all combustion mixtures (Table 1) and, since excellent reproducibility was observed among the different records, hereafter only the smoothed data will be presented.

Results and Discussion

Formation of soot particles

C_2H_2/O_2 flames with C/O ratio = 0.65 (mixture 1) and C/O ratio = 0.75 (mixture 2) presented no expressive

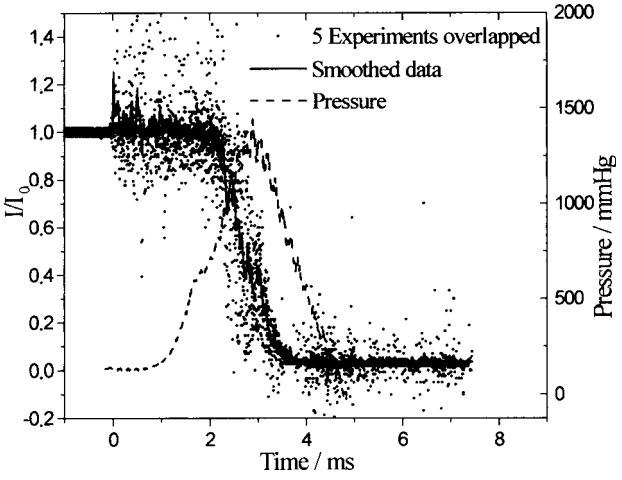

Figure 2. Overlapping of five laser extinction records of five independent C_2H_2/O_2 combustion processes with C/O ratio = 1.00 (mixture 5). The solid line is the smoothed data for laser extinction. The dashed line shows the smoothed pressure increase and subsequent decrease during the combustion process.

reduction of laser intensity. On the other hand, C_2H_2/O_2 flames with C/O ratio > 0.75 show very intense laser extinction during combustion. Hence, the C/O ratio = 0.75 is a lower limit for soot formation.

Soot grows through nucleation, superficial growth and coalescence of the particles. Figure 2 shows the total soot formation process and the pressure change inside the chamber for combustion of mixture 5 (Table 1). The pressure rises significantly before of the detection of soot particles with sizes large enough for laser beam extinction (from 0 to 2 ms). This pressure increase is held for around 3 ms. After the end of soot formation, the pressure decreases to values near the initial ones (ca. 4.5 ms).

Pressure exerts a large influence on the temporal behavior of soot formation[9] and the results in Figure 2 indicate that the pressure increase mainly affects the beginning of the soot formation process (from 0 to 2 ms), probably the nucleation step.

Figure 3 shows the temporal behavior of laser intensity as consequence of soot particle formation during C_2H_2/O_2 and C_2H_2/O_2/Ar combustion processes for mixtures 3-6. The temporal behavior of soot formation is very similar for the different flames. After an induction time for reaction of about 2 ms, all of them show an abrupt transmittance decrease until the laser light is fully extinct ($I/I_0 = 0$). The induction time is probably related to the nucleation process of the soot production mechanism. After the nucleation around 1.0-2.0 ms, for the C_2H_2/O_2 and C_2H_2/O_2/Ar flames, there is rapid soot formation, as indicated by the abrupt laser signal reduction. The total soot formation phenomenon in the flames studied in a closed chamber lasts 3.0-4.0 ms, as shown in Figure 3. However, the chemiluminescence and pressure changes are still detected until around 4.0-4.5 ms, as indicated in Figure 4.

The chemiluminescence of excited radicals and the pressure change of gas mixtures under combustion reached a maximum simultaneously. The maxima occur approximately at the end of the soot formation process in the C_2H_2/O_2 and C_2H_2/O_2/Ar flames with C/O ratio = 1.00.

The total time of soot formation in atmospheric laminar flames has been estimated to be around 10-30 ms,[9,11] with the initial 2-3 ms due to the nucleation step.[9] Our results show that soot chemistry in closed chamber combustion may be different, mainly in surface growth or coalescence steps, which are faster than those in open system combustion.

Figures 5 and 6 show micrographs of compact and almost spherical soot particles with 60-150 nm diameters and aggregates collected about five seconds after the combustion reactions of C_2H_2/O_2 and C_2H_2/O_2/Ar with C/O ratio = 1.00, respectively.

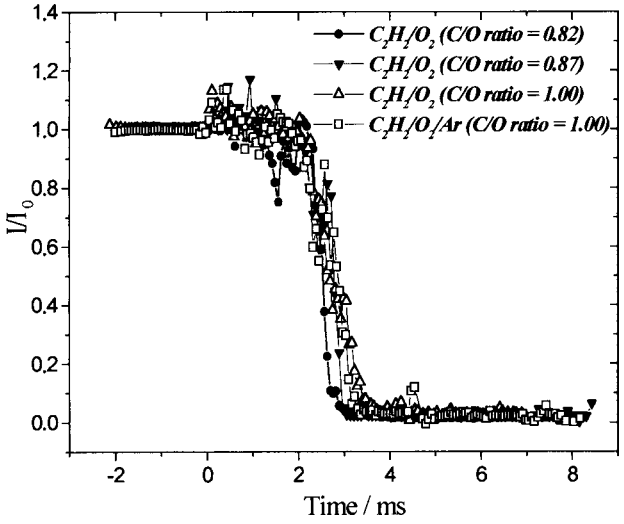

Figure 3. Temporal evolution of soot formation in the C_2H_2/O_2 with different C/O ratios (mixtures 3, 4 and 5) at initial pressures of 140 mmHg and temporal evolution of soot formation in C_2H_2/O_2/Ar with C/O ratio = 1.00 at initial pressure of 210 mmHg.

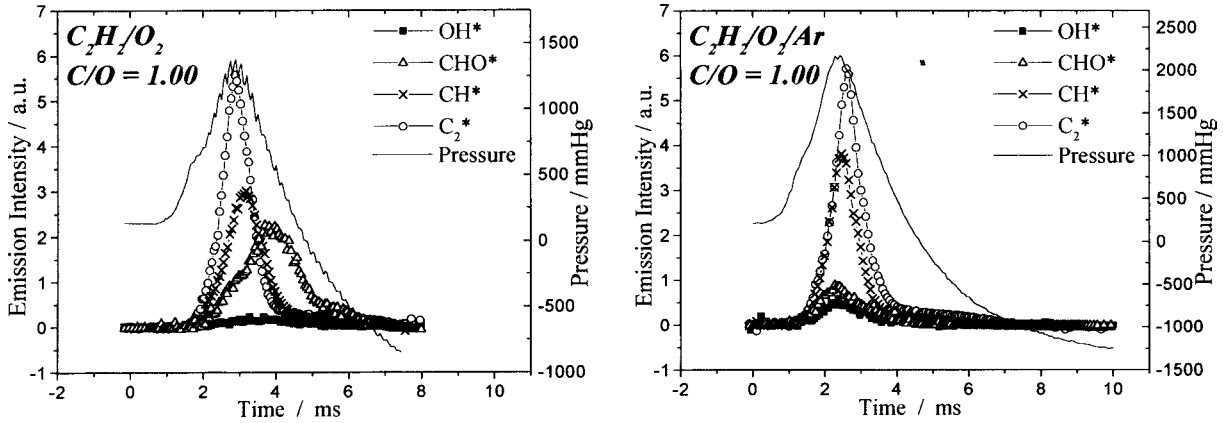

Figure 4. Chemiluminescence of OH*, CHO*, CH* and C_2* excited radicals and pressure evolution from C_2H_2/O_2 (mixture 5) and C_2H_2/O_2/Ar (mixture 6) flames with C/O ratio = 1.00.

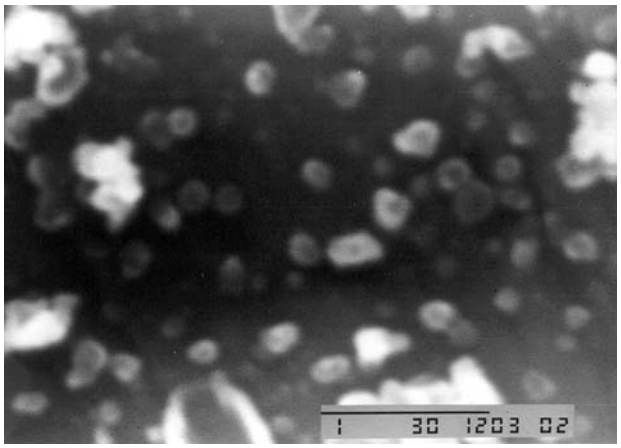

Figure 5. Scanning electronic microscopy (SEM) of soot particles and aggregates from C_2H_2/O_2 with C/O ratio = 1.00 at an initial pressure of 140 mmHg, sampled five seconds after the reaction. Bar length = 1 μm (35000X).

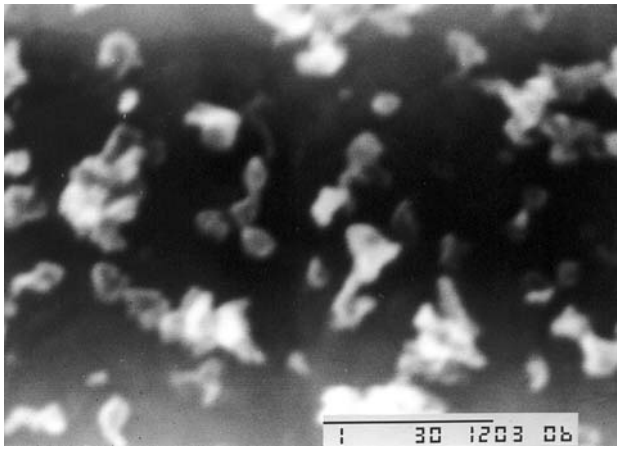

Figure 6. SEM of soot particles and aggregates from C_2H_2/O_2/Ar with C/O ratio = 1.00 at an initial pressure of 210 mmHg, sampled five seconds after the reaction. Bar length = 1 μm (35000X).

Although argon addition does not change the time behavior of chemiluminescence or the pressure change and practically does not change the total time of soot formation, the morphology of the primary soot particles was changed (Figure 6), indicating a modification of the surface growth and coalescence mechanism. For the C_2H_2/O_2/Ar flame (Figure 6), one can observe predominantly aggregates and the soot particles are less spherical.

Studies have shown that the earliest formed particles, which are considered to be the precursors of soot, have typical sizes of about 2-3 nm.[7,8] Our results show that after only few milliseconds these small particles have grown rapidly, reaching 60-150 nm (Figure 5 and 6).

By considering that soot particles are approximately spherical, the soot volume fraction (f_v) can be evaluated by:[25]

$$f_v = \frac{-\ln(\tau_\lambda)\lambda}{k_\lambda s} \quad (1)$$

where τ_λ is the measured transmittance, λ is the wavelength of laser light emission, k_λ is the absorption coefficient per unit of volume fraction of soot (4.892 at 632.8 nm)[25] and s is the uniform sample volume path length.

Figure 7 shows the soot volume fraction as a function of time calculated from the laser extinction of the combustion processes. The soot volume fraction data refer to the mean value, since the laser crosses the entire combustion chamber. The soot volume fraction from laser extinction ($I/I_0 = 0$) was measured up to 3 ppm, as the upper limit of detection of our system. This limit value was reached in the time interval of 3.0-4.0 ms for all the flames studied and presents the same magnitude as that observed at several different flame regions in a large fuel pool fire experiment[25] and in laminar / turbulent flames.[2,9]

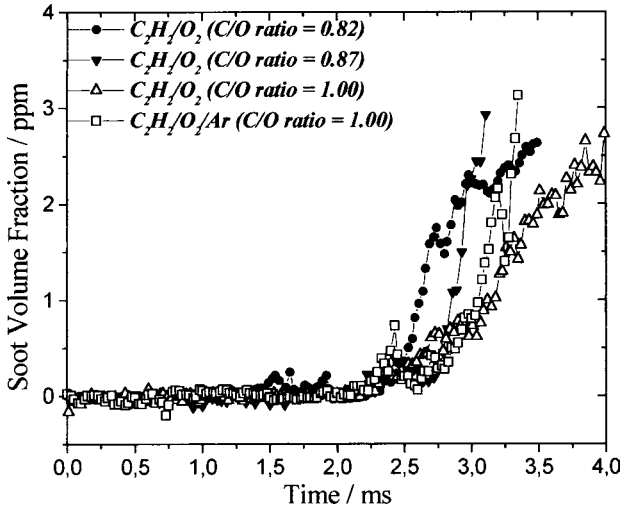

Figure 7. Soot volume fractions as a function of time for C_2H_2/O_2 flames with different C/O ratios at initial pressures of 140 mmHg and a C_2H_2/O_2/Ar flame with C/O ratio = 1.00 at an initial pressure of 210 mmHg.

The soot volume fraction for the combustion of all mixtures studied changes as a function of time, resulting in different velocities of soot formation, as indicated in Figure 7. The fuel-richest C_2H_2/O_2 mixture (C/O ratio = 1.00) has a slower velocity and argon addition to C_2H_2/O_2 mixture increases the velocity of soot formation.

The higher velocity of soot formation in the C_2H_2/O_2/Ar flame could be explained by the reduction of flame temperature caused by argon addition. Argon could dilute the combustion mixture changing the reaction steps of growth of species of high molecular mass (PAHs) to soot. As reported by Takahashi and Glassman[26] at lower

temperature the soot precursors production increases and their oxidation decreases. The argon addition also changes the morphology of particles as indicate in Figure 6.

Soot aggregation

Soot aggregation occurs after the final soot particle formation. This means that the aggregation process occurs in another time domain and its kinetics is much slower than particle formation and growth.

The aggregation of the soot formed in C_2H_2/O_2 and C_2H_2/O_2/Ar flames with C/O ratio = 1.00 was monitored by the laser intensity change after reaction. Soot particles in these processes are confined in the closed chamber until complete aggregation.

Figure 8 shows the transmittance enhancement that could be correlated to soot aggregation as a function of time for mixtures 5 and 6. The total aggregation time of soot particles formed in the C_2H_2/O_2/Ar combustion was about 20 min while in the C_2H_2/O_2 combustion it was approximately 12 min.

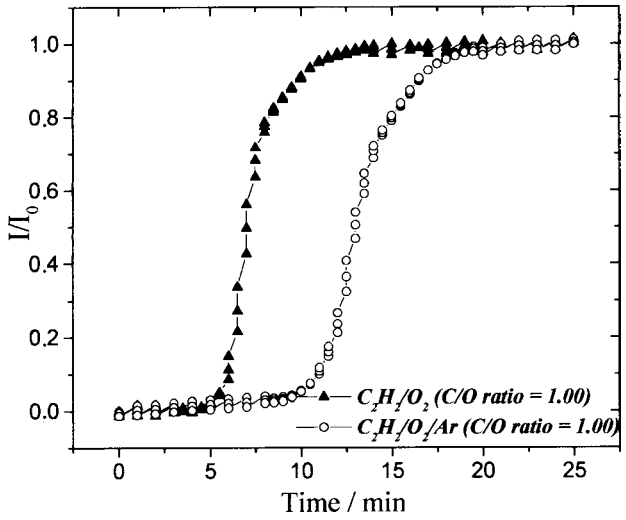

Figure 8. Soot aggregation as a function of time in the C_2H_2/O_2 and C_2H_2/O_2/Ar flames with C/O ratio = 1.00.

To evaluate the morphology of aggregates formed in the aggregation process, soot aggregates were collected at different times after the C_2H_2/O_2 combustion with C/O ratio = 1.00. Figures 9, 10 and 11 show micrographs of soot aggregates collected 1, 15 and 30 min after the reaction, respectively.

Aggregates collected 1 min after the C_2H_2/O_2 combustion (Figure 9) are dispersed over the sample holder surface and they are composed of particles whose morphology and sizes resemble the isolated particles collected 5 sec after the reaction (Figure 5).

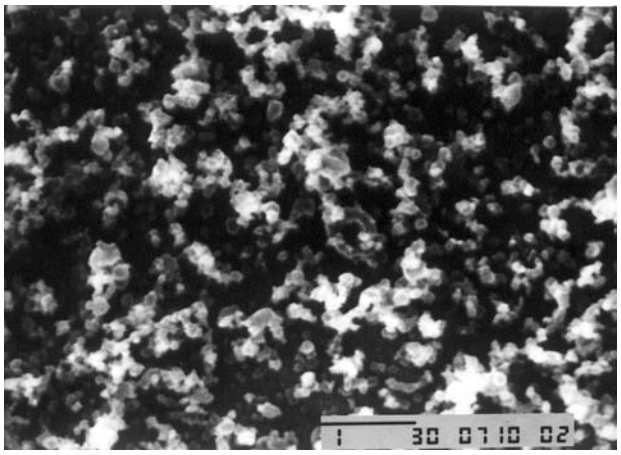

Figure 9. SEM of soot aggregates from C_2H_2/O_2 with C/O ratio = 1.00 at an initial pressure of 140 mmHg, sampled 1 minute after the reaction. Bar length = 1 μm (20000X).

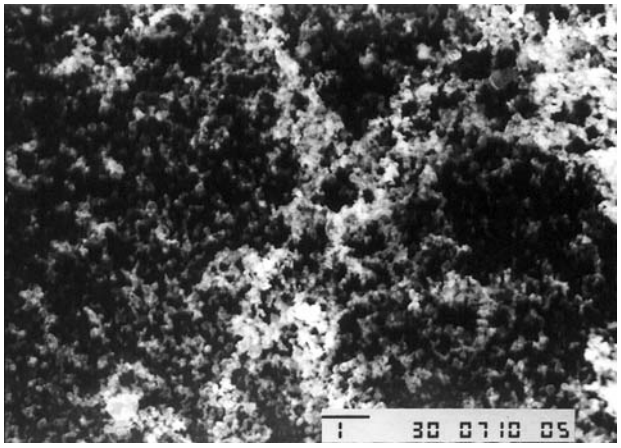

Figure 10. SEM of soot aggregates from C_2H_2/O_2 with C/O ratio = 1.00 at an initial pressure of 140 mmHg, sampled 15 minutes after the reaction. Bar length = 1 μm (10000X).

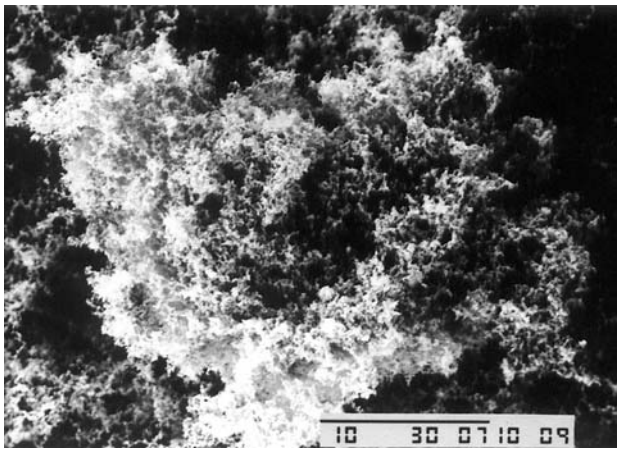

Figure 11. SEM of soot aggregates from C_2H_2/O_2 with C/O ratio = 1.00 at an initial pressure of 140 mmHg, sampled 30 minutes after the reaction. Bar length = 10 μm (3500X).

Spherical soot particles produce aggregates of increasing sizes and the continuous deposition of the aggregates over the sample holder along with time results in a netlike structure, not compacted and similar to that of an aerogel.

Conclusions

There is intense soot formation during short periods of time for flames from C_2H_2/O_2 with C/O ratio > 0.75 and C_2H_2/O_2/Ar with C/O ratio = 1.00 in a closed chamber. The total time of soot formation in these flames was found to be about 3.0-4.0 ms.

The chemiluminescence of radicals and the pressure change reached a maximum simultaneously and at approximately the final stage of the soot formation process. The pressure increase has significant influence on the nucleation step of soot formation.

The soot formation mechanism in a closed chamber probably differs from that in open systems, mainly in surface growth or coalescence steps, which are faster for the closed system.

The soot precursors grow quickly, reaching compact and almost spherical primary particles, with diameters of 60-150 nm for C_2H_2/O_2 and C_2H_2/O_2/Ar flames with C/O ratio = 1.00 within milliseconds. The addition of argon to the C_2H_2/O_2 mixture changed the morphology of the soot particles and the velocity of soot formation. It was found that the velocities of soot formation are slower for the fuel-richest C_2H_2/O_2 mixture (C/O ratio = 1.00) while argon addition to the C_2H_2/O_2 mixture increases the velocity of soot formation.

The compact and almost spherical soot particles produce aggregates of increasing sizes. The total aggregation time of soot particles formed in the C_2H_2/O_2/Ar combustion was about 20 min while in the C_2H_2/O_2 combustion it was approximately 12 min.

Acknowledgements

This work was supported by FAPESP (Fundação de Amparo à Pesquisa do Estado de São Paulo) through projects 96/09627-9 and 97/07938-0.

References

1. Sorensen, C. M.; Feke, G. D.; *Aerosol Sci. Technol.* **1996**, *25*, 328.
2. Koylu, U. O.; McEnally, C. S.; Rosner, D. E.; Pfefferle, L. D.; *Combust. Flame* **1997**, *110*, 494.
3. Kittelson, D. B.; *J. Aerosol Sci.* **1998**, *29*, 575.
4. Xu, F.; Lin, K. C.; Faeth, G. M.; *Combust. Flame* **1998**, *115*, 195.
5. Wellmünster, P.; Keller, A.; Homann, K. H.; *Combust. Flame* **1999**, *116*, 62.
6. Bartenbach, B.; Leuckel, W.; *Twenty-Sixth Symposium (Int.) on Combustion*, The Combustion Institute, Napoli, Italy, 1996.
7. Minutolo, P.; Gambi, G.; D'Alessio, A.; *Twenty-Seventh Symposium (Int.) on Combustion*, The Combustion Institute, Boulder, USA, 1998.
8. D'Alessio, A.; D'Anna, A.; Gambi, G.; Minutolo, P.; *J. Aerosol Sci.* **1998**, *29*, 397.
9. Said, R.; Garo, A.; Borghi, R.; *Combust. Flame* **1997**, *108*, 71.
10. Chomiak, J. In *Combustion, a Study in Theory, Fact and Application*, Gordon and Breach Science Publishers; Montreaux, 1990, p. 311.
11. Randy, L.; Wal, V.; Ticich, M.; Stephens, B.; *Combust. Flame* **1999**, *116*, 291.
12. Calcote, H. F.; *Combust. Flame* **1981**, *42*, 215.
13. Saito, K.; Gordon, A. S.; Williams, F. A.; Stickle, W. F.; *Combust. Sci. Technol.* **1991**, *80*, 103.
14. Peeters, J.; *Bull. Soc. Chim. Belg.* **1997**, *106*, 337.
15. Sivathanu, Y. R.; Gore, J. P.; *Combust. Sci. Technol.*, **1991**, *80*, 1.
16. Greenberg, S. P.; Ku, J. C.; *Appl. Opt.* **1997**, *36*, 5514.
17. Wal, R. L. V.; *Combust. Sci. Technol.* **1996**, *118*, 343.
18. Unkhoff, M. B.; Chrysostomou, A.; Frank, P.; Gutheil, E.; Lückerath, R.; Stricker, W.; *Twenty-Seventh Symposium (Int.) on Combustion*, The Combustion Institute, Boulder, USA, 1998.
19. Axelsson, B.; Collin, R.; Bengtsson, P. E.; *Appl. Opt.* **2000**, *39*, 3683.
20. Dobbins, R. A.; Megaridis, C. M.; *Langmuir* **1987**, *3*, 254.
21. Koylu, U. O.; Faeth, G. M.; *Combust. Flame* **1992**, *89*, 140.
22. Glassman, I.; Sidebotham, G. W.; *Combust. Flame* **1992**, *90*, 269.
23. Gaydon, A. G. In *The Spectroscopy of Flames*. John Wiley & Sons; New York, 1974, p. 338.
24. Bertran, C. A.; Marques, C. S. T.; Benvenutti, L. H. *Combust. Sci. Technol.*, in the press.
25. Gritzo, L. A.; Sivathanu, Y. R.; Gill, W.; *Combust. Sci. Technol.* **1998**, *139*, 113.
26. Takahashi, F.; Glassman, I.; *Combust. Sci. Technol.* **1984**, *37*, 1.

Received: November 8, 2000
Published on the web: October 11, 2001

FAPESP helped in meeting the publication costs of this article.